



Original Article

Validation of a Football Helmet Finite Element Model and Quantification of Impact Energy Distribution

M. A. CORRALES, D. GIERCZYCKA, J. BARKER, D. BRUNEAU, M. C. BUSTAMANTE, and D. S. CRONIN 

Department of Mechanical and Mechatronics Engineering, University of Waterloo, 200 University Ave. West, Waterloo, ON N2L 3G1, Canada

(Received 24 May 2019; accepted 9 September 2019; published online 23 September 2019)

Associate Editor Joel D Stitzel oversaw the review of this article.

Abstract—Head injury in contact sports can be mitigated, in part, through the enhancement of protective helmets that may be enabled by detailed finite element models. However, many contemporary helmet FE models include simplified geometry and material properties and have limited verification and validation over a representative range of impact conditions. To address these limitations, a detailed numerical model of a modern football helmet was developed, integrated with two headforms and assessed for 60 impact conditions with excellent ratings (0.79–0.93). The strain energy of the helmet components was investigated for eight impact locations and three impact speeds. In general, the helmet shell had the highest strain energy followed by the compression shocks; however, the facemask and straps had the highest strain energy for impacts involving the facemask. The component strain energy was positively correlated with the Head Injury Criterion, while the strain energy was not strongly correlated with the Brain Injury Criterion due to the dependence on rotational kinematics. This study demonstrated the applicability of a detailed football helmet finite element model to investigate a range of impact conditions and to assess energy distribution as a function of impact location and severity as a means of future helmet optimization.

Keywords—Impact, Head injury, Anthropomorphic test device, Helmet design.

INTRODUCTION

Traumatic brain injury (TBI) sustained by athletes occurs at the highest rate in American football (6.4 per 10,000 athletics exposure) with high concussion rates

at the high school, collegiate¹⁰ and the professional levels of play²⁵ and accounts for 47.1% of sport-related concussions.¹⁹ Considering head impacts in American football, the helmet is the primary energy absorbing component, with the aim to reduce head kinematics. Since a combination of linear and rotational kinematics^{12,16,17,21,26,29} has been hypothesized to cause concussive neurotrauma,⁴⁰ head angular velocity and linear acceleration are commonly used to evaluate football helmet performance. The National Operating Committee on Standards for Athletic Equipment certification standard^{22,36} limits allowable linear accelerations in a drop test impact with a rigid neck. The Summation of Tests for the Analysis of Risk (STAR) rating system²⁸ uses peak angular velocities to determine the helmet performance (1 to 5 stars) using the Hybrid III head and deformable neck with four head impact locations. In general, helmets with lower angular kinematics measured at the head center of gravity (COG) perform better on the STAR evaluation system. However, it has been suggested that test apparatus allowing head rotational displacements and including a broader combination of impact locations and speeds could improve helmet assessment.¹² This is, in part, related to the finding that concussions are associated with specific impact directions and that different types of impact are associated with the varying player position.³⁶ The linear impact test²³ evaluates the helmet in a wide variety of impact locations and speeds, and the incorporation of a deformable Hybrid III head-and-neck assembly enables the assessment of angular kinematics. The linear impact test will be adopted by NOCSAE²⁴ for helmet evaluation in 2019.

Address correspondence to D. S. Cronin, Department of Mechanical and Mechatronics Engineering, University of Waterloo, 200 University Ave. West, Waterloo, ON N2L 3G1, Canada. Electronic mail: duane.cronin@uwaterloo.ca

Finite element (FE) models have been used as a research tool to investigate the structural and kinematic response to impact, and to a lesser extent to evaluate and optimize protection design. Detailed FE models, which are validated under a wide range of impact conditions, have the potential to enhance the performance of current protection by providing information that would be challenging to retrieve by laboratory methods; namely video analysis,²⁶ in-game accelerometer data,^{6,32} physical helmet experiments,^{35,38} and physical component level experiments.^{2,4} The understanding of the behaviour of energy absorbing components is of interest at the stage of designing helmets, evaluating their performance, and in reducing head injury risk. Johnston *et al.*¹⁵ developed a football helmet FE model (Schutt Ion 4D) to investigate changes of performance due to numerical alteration of energy absorbing padding within the helmet model. Both the physical helmet and the numerical equivalent were donned on a NOCSAE headform²³ coupled with a rigid neck, subjected to drop test impacts (heights of 304.8 mm to 1524 mm), and lateral linear impacts (velocity between 3.2 and 3.3 m/s) where axial rotation of the head was allowed. Although this study demonstrated the potential for FE models to provide information on helmet performance, no details were provided for: the headform model and validation, the geometry development of the helmet model, or model validation were provided.

In another study, Johnson *et al.*¹⁴ integrated a simplified generic football helmet FE model with a simplified human head FE model comprising three components (skull, cerebrospinal fluid, and brain) to perform a topological optimization on the helmet facemask. The optimization-targeted reduction of shear strain and maximum tensile pressure predicted in the FE brain model under a linear impact. However, no details on the helmet or head model validation were provided.

Darling *et al.*⁵ integrated an FE model of a current American football helmet (Riddell Attack Revolution Youth helmet) with the Global Human Body Models Consortium (GHBMC 2014) average stature male Human Body Model (HBM) to evaluate TBI risk under helmeted and non-helmeted head impacts. The FE helmet model geometry was based on the youth football helmet (Riddell Attack Revolution Youth) and simplified to comprise the shell, a uniform foam energy absorbing layer, and a uniform soft foam comfort liner. A linear elastic constitutive model was used for the helmet shell, whereas a non-linear and non-strain rate-dependent constitutive model was used for energy absorbing and comfort foam layers. The physical helmet was assessed using a low-severity (3 m/s) experimental drop test, where the helmet was donned on a

hemispherical cap representing the headform in a non-standard test configuration impacting the crown of the helmet. The integrated FE HBM-helmet assembly was subjected to crown, and frontal (forehead) impacts to investigate brain response. However, the responses were only tracked for 20 ms, which corresponded to the initial portion of the loading phase.⁵ Due to the considered impact direction, the helmet model did not contain the facemask, chin cup, and a strap system. Other previous studies have focused on energy attenuation of football helmets fitted on headforms^{7,39} or focused on the energy attenuation of helmet liner components in isolation.^{13,18} However, no previous studies have quantified the energy distribution of the individual helmet components over a representative range of impacts conditions, and most studies have focused only on the helmet liner materials, but have generally not considered the helmet shell, facemask and chin straps.

Giudice *et al.*¹¹ developed an open source set of headforms and impactors based on NOCSAE and STAR protocols,^{23,28} namely the NOCSAE head, and HIII head and neck models. Typical impact boundary conditions were also developed including the drop test, linear impactor, and pendulum impactor. Giudice *et al.*¹¹ validated the FE models against 20 commonly used load cases for helmet evaluation, subjecting the HIII head and neck, and NOCSAE headform to the linear impactor, pendulum, and drop test loading. The models were compared to the experiments using International Organization for Standardization (ISO)¹ and CORrelation and Analysis (CORA)⁹ cross-correlation methods, where a rating of 0 means no correlation and 1 means strong correlation between the measured experimental data and the simulation response. The models achieved good ISO cross-correlation [0.65–0.81], and good to excellent CORA ratings [0.71–0.89]. Recently, a set of 240 linear impactor, drop tower and pendulum impact experiments using four modern football helmets (60 experiments per helmet) donned on the NOCSAE and HIII headforms was published³ under the NFL engineering road map,³⁷ providing a valuable data set for assessing the performance of FE helmet models.

Within the present study, a detailed FE model of a modern football helmet (Xenith X2E 2016, Fig. 1b) comprising the compression shocks (thermoplastic polyurethane (TPU)), helmet shell (polycarbonate), face mask (steel coated by polyurethane), shock bonnet (TPU), comfort pads (bilayer of high and low density foam encapsulated in vinyl) (Fig. 1a), was developed to assess helmet performance, quantify the strain energy per component, identify potential areas for improvement, and optimize future helmet designs. FE models of the helmet components (helmet shell, face-

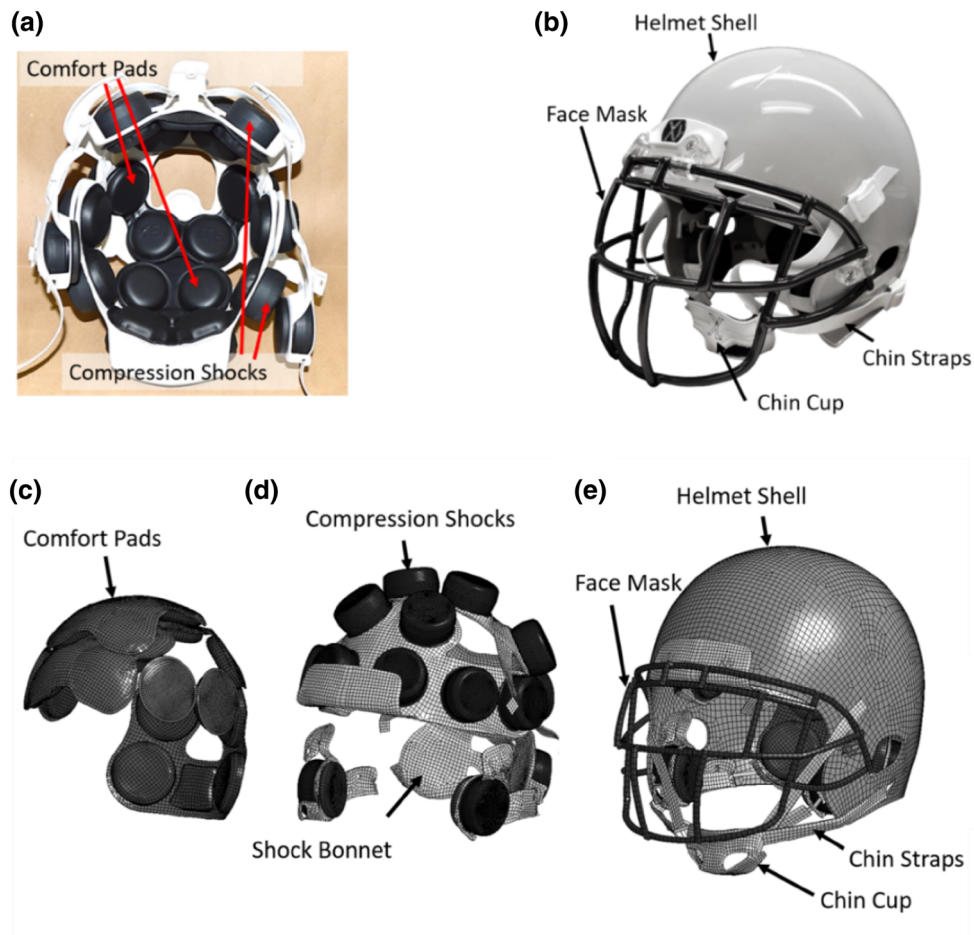


FIGURE 1. Modern American football helmet (Xenith X2E) incorporating energy absorbing components.

mask, compression shocks, comfort pads, straps) were previously developed and validated.^{2,4} Material samples were extracted from the helmet and tested at quasi-static and dynamic rates (0.01 to 1400 s^{-1}), in a loading mode corresponding to the component function in the helmet, and the isolated components were tested in the primary mode of loading seen in an impact scenario (e.g., compression shock and comfort pads were tested in through-thickness compression) at quasi-static and dynamic rates (0.0002 to 120 s^{-1}). Constitutive models were identified and implemented based on the material test data for validation of the components with the experimental data, demonstrating good (0.65 to 0.85) to excellent (0.86 to 1) CORA ratings (0.95 – 0.98 , 0.93 , 0.94 – 0.97 , and 0.85 – 0.96 for the helmet shell, facemask, compression shocks, and comfort pads, respectively). Mesh sensitivity studies were previously performed on the individual helmet components⁴ and were found to be within 2 to 7% of the theoretical zero mesh size.²⁷

In this study, the helmet components were assembled into a full helmet FE model and donned on HIII

and NOCSAE head FE models.¹¹ The assembled helmet model was extensively validated using 60 physical impact experiments³ and the helmet model was used to assess the component energy distribution for varying impact velocity and location.

MATERIALS AND METHODS

The physical helmet (X2E 2016, Xenith, LLC, size large) (Fig. 1b) was scanned using Computer Tomography (CT) (General Electric Phoenix-V|tome|x-s, 2014) in the fully assembled form to provide a reference for the assembled helmet model. The helmet was then disassembled into individual components (helmet shell, facemask, chin cup and straps, shock bonnet suspension system with compression shocks, and foam comfort pads) (Fig. 1). The individual components were then scanned and processed into surfaces using Geomagic Wrap (3D Systems, Rock Hill, SC), which were then meshed using HyperMesh 14.0 (Altair Engineering, Inc., Troy, MI).

Helmet Model Assembly

The facemask was fixed to the helmet shell (Fig. 1e) at four locations using rigid beams representing clips in the physical helmet (Fig. 1b). The compression shocks (Fig. 1d) were integrated with the shock bonnet (Fig. 1d) through tying edges of the shocks to the bonnet using a nodes-to-surface contact algorithm to model the thermal joining between the components. Since the reference surfaces for the shock bonnet mesh were CT-scanned for a disassembled component, separate from the helmet shell, a pre-simulation was required to integrate the bonnet within the helmet shell. To locate the bonnet within the shell, the helmet shell was treated as rigid and kept stationary, while the bonnet and compression shocks were assigned physical material properties. The shock bonnet mesh was located inside the helmet shell, and a NOCSAE headform with prescribed motion was used to push the bonnet components to the final locations. The target location was confirmed using the full helmet scan, and physical helmet. The separate jaw compression shocks were positioned inside the helmet shell through graphical pre-processing (LS-PrePost 4.5, Livermore Software Technology Corporation, US), matching their final location in the assembled helmet. A fit was achieved when the bonnet and compression shock location matched the assembled helmet scan locations, ensuring there was no deformation of the shocks due to contact with the helmet shell. Tied contacts were used to represent screws connecting the bonnet to shell in the physical helmet.

The foam comfort pads (Fig. 1c) were scanned, segmented, and meshed as individual components; therefore, they were required to be fitted inside the shock bonnet to match their final positions. For the fitting process, the foam materials and corresponding vinyl covers were assigned elastic material properties with high stiffness (20 times the actual material properties) to avoid deformation of the foam during initial positioning. The NOCSAE headform with prescribed motion was used to move the comfort pad models to the target locations in the assembled physical helmet (Fig. 1b). Tied contacts were then used to connect the comfort pads to the shock bonnet (Fig. 1d), representing the Velcro connections in the physical helmet.

The strap system was modelled using shell elements at locations where the straps could contact the headform, and with 1D tension-only elements otherwise to numerically simplify guiding the straps through eyelets of the shock bonnet suspension system. This approach was adapted from seatbelt modelling practices in the automotive industry.³⁴ The chin cup was positioned in the vicinity of the chin, based on images of a helmet donned on a headform. To ensure that helmet straps

remain tightened, seatbelt retractor elements were included in the model at four locations corresponding to clips connecting straps to shell in the physical helmet. Prior to an impact simulation, the retractor elements were activated and applied an initial tension of 50 N per side to represent the strap pretension in a helmet donned on the headform or worn.

Donning the Helmet Model on the Headform

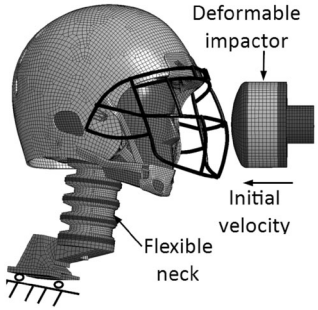
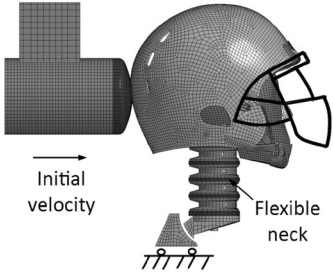
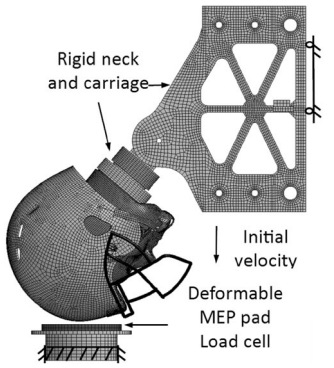
The helmet model was donned on the NOCSAE and HIII headform models developed by Giudice *et al.*¹¹. Firstly, the headform and helmet models were overlaid in a graphical pre-processor (LS-PrePost 4.5) in accordance with the experimental tests (Biocore LLC). The helmet shell and facemask nodes were then constrained in all directions, and the headform was initially uniformly scaled down to 75% of the original size, to fit inside the helmet assembly without contacting any components, and then expanded uniformly until it reached full size through pre-simulation. All components of the helmet were assigned the average reported material properties⁴ to ensure a realistic fit between the headform and the deformable internal components of the helmet. A final pre-simulation was conducted to position the chin cup and adjust the straps around the coupled head-helmet model to match the position of the helmet relative to the head as reported in the experiments. The process was conducted for both the HIII and NOCSAE headforms separately to account for their specific geometry. The integrated helmet and headform models were then subjected to impact scenarios and assessed using the corresponding experimental data.

Helmet Model Validation for 60 Impact Cases

The helmet finite element model was analyzed using a commercially available explicit finite element solver (LS-DYNA, version R7.1.2). The pre and post processing was done in LS-PrePost (v4.2, LSTC, Livermore, CA, USA) and custom scripts to process the data were written in VBA (Excel, Microsoft, Santa Monica, CA, USA). Details on the constitutive models, contact algorithms and element types within the helmet model are included in the supplemental material (Table S8) and can be found in the publically available helmet model.³⁷

Sixty experimental tests (Table 1) performed on the physical Xenith X2E helmet in a laboratory environment^{3,11} were used to validate the numerical helmet model. The experimental tests were performed following the NFL helmet test protocol⁸ and STAR rating system³⁰ standards, namely a linear impactor and pendulum impacts including the HIII head and neck

TABLE 1. Summary of helmet impact boundary conditions.

Impactor type	Linear impactor	Pendulum	Drop test	
				
Headform	HIII	HIII	HIII	NOCSAE
Loading direction	Low facemask, oblique facemask, side facemask, side, rear oblique, front, rear, low side	Rear oblique, front top, side oblique, side	Rear, front, side oblique, top	Front, side, top
Velocity (m/s)	5.5, 7.4, 9.3	3.0, 4.6, 6.1	2.9, 4.9, 6.0	2.9, 3.7, 4.9 6.0

assembly, and a drop test impact with the use of two headforms (NOCSAE, and HIII head and neck) at different impact velocities and directions. For the drop test configurations, an initial velocity was applied to the parts that were in motion: helmet, headform, and the drop test carriage. The motion of the base of the deformable Modular Elastomer Programmer (MEP) pad and the load cell was constrained in all directions. The initial velocity applied to the parts in motion represented the velocity at the moment before impact for four different drop tests with the NOCSAE headform (2.9, 3.7, 4.9, and 6.0 m/s) and three with the HIII headform (2.9, 4.9, and 6.0 m/s). Headform kinematics, carriage kinematics, and load cell force were extracted from the model simulations. For the pendulum (3.1, 4.6, and 6.1 m/s) and linear impactor (5.5, 7.4, and 9.3 m/s) models, the initial velocity was applied to the impactor only. The deformable model of the helmet, head and neck were free to move following the impact, as in the experimental test set up (Table 1).

Headform kinematics, impactor kinematics, and impactor load cell force predicted by the model were compared to the experimental data and assessed objectively using cross-correlation. The drop tests did not allow for head rotation, and the pendulum test series did not include a force transducer in the pendulum impactor. Therefore, these metrics were not incorporated into the CORA cross-correlation rating assessment. A list of the metrics used for the model validation can be found in the Supplementary Material (Table S1).

The termination time for all simulations was set to 50 ms, which was well beyond that required for analysis of the relevant kinetics and kinematics. The loading and unloading phases of the impacts, and relevant kinematics, were all complete by a time of 30 ms, and so this was the timeframe used for the CORA analysis. The experimental curves and model results for a given impact case were synchronized in time using the initial rise of the impactor acceleration trace from the experiments and impactor acceleration trace from the model (Fig. 2d). The same synchronization or time shift was applied to all model data. The weighting factors for the shape, size, and phase ratings were 0.5, 0.25, and 0.25 respectively, and the maximum allowable phase shift was 4.5 ms (15%) for each signal comparison. The phase rating was equal to 1 if the phase shift was less than 0.3 ms (1%), and equal to 0 if the shift was greater than 3.0 ms (10%). The CORA ratings for the three components of head translational acceleration and rotational velocity were combined into one rating each using the Signal Magnitude Factor³¹ based on the experimental peak magnitude.

In addition to the measured head kinematics, for the linear impactor load case, the rotation of the helmet shell in the XZ plane was extracted from the experimental videos and compared to the model rotation response using CORA. A video analysis package (Tracker v4.96), was used to measure the position of two landmarks in the video, and the same two landmarks were used to calculate the rotation of the helmet

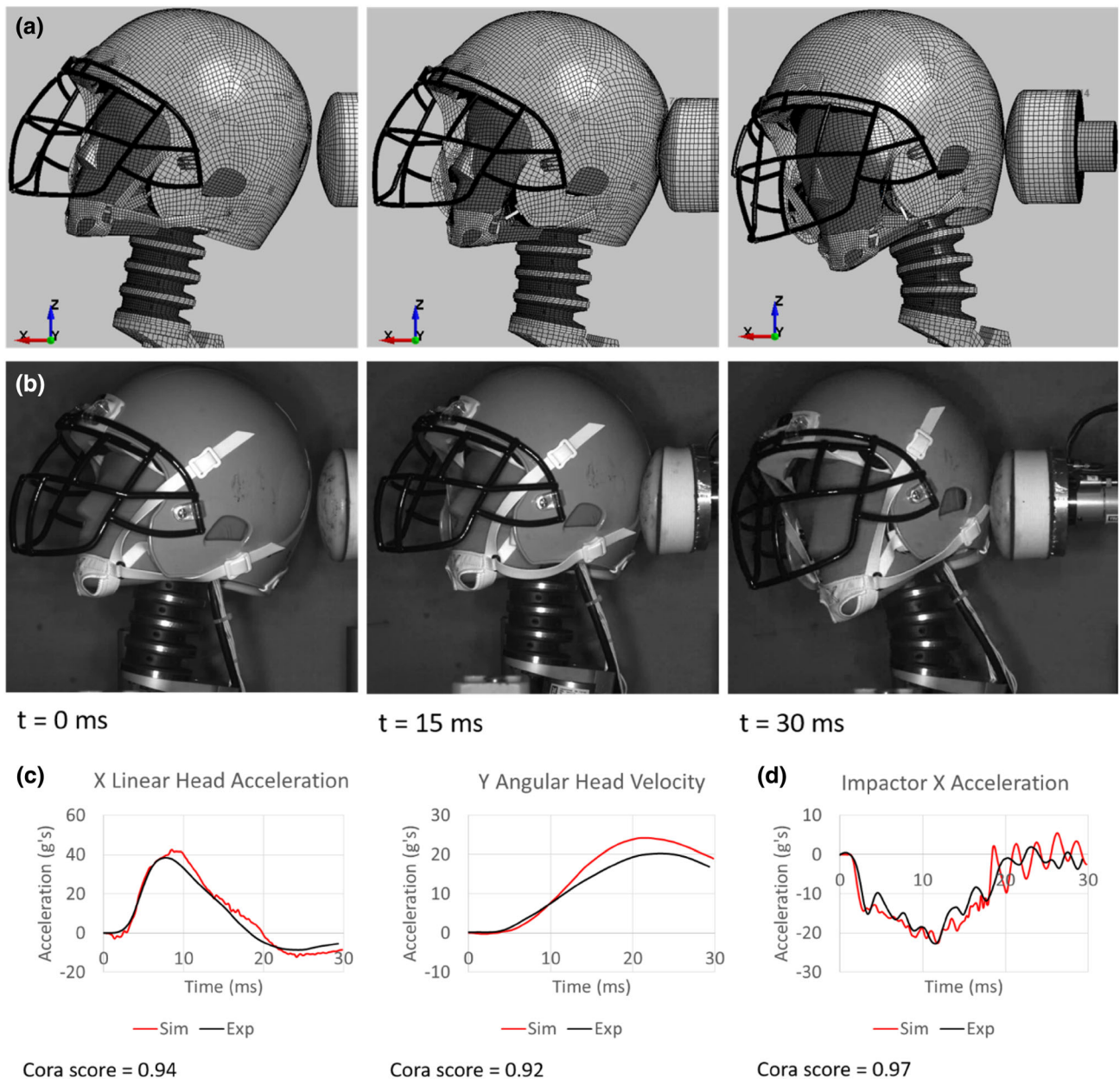


FIGURE 2. Linear impactor rear oblique configuration at 5.5 m/s. (a) simulation, (b) experiment video, (c) experimental (black) and simulation (red) plots of the head kinematics in the impact direction and (d) impactor kinematic used for signal alignment.

in the model. The location of the landmarks can be found in the Supplementary Material (Fig. S1).

Strain Energy Distribution in Helmet Component Groups

The linear impactor test evaluated the helmet over a wide range impact speeds and locations; hence, the strain energy or internal part energy of each component was extracted from the model (LS-PrePost, Internal energy in the matsum database) for these load cases. The helmet was assessed in five component

groups: helmet shell, compression shocks, facemask, straps system, and comfort pads. The total strain energy of each group was defined as the sum of the strain energy of all components within the group (e.g., the strain energy of the compression shocks was defined as a sum of strain energy of each shock in the helmet at a given time step). The total energy of the comfort pads was the sum of the total strain energy of the foam and the vinyl cover, where the vinyl accounted for no more than 3% of the total strain energy. The total strain energy of the helmet was calculated by summation of the strain energy of the five energy absorption groups,

and the contribution of each group to the total helmet strain energy was calculated as a percentage, that is group strain energy divided by the total helmet strain energy. The potential for head injury risk was evaluated by calculating the Head Injury Criterion (HIC_{15})²⁰ based on resultant linear head acceleration for each impact scenario, and Brain Injury Criterion (BrIC),³³ based on maximum head rotational velocities. Correlation of the HIC_{15} and BrIC values with strain energy in the five groups of components was then evaluated. A linear regression and Spearman's correlation were used to identify the presence and strength of positive or negative correlation.

RESULTS

Helmet Model Validation for 60 Impact Cases

The CORA ratings obtained for the head and impactor kinematics (Table 2) varied from good (0.65 to 0.85) to excellent (0.86 to 1), where the drop test cases had the highest ratings, 0.88 with the HIII headform and 0.93 with the NOCSAE headform, while the linear impactor had a rating of 0.82 and the pendulum impact 0.83. The model response for helmet rotation was in good agreement with the experimental data measured from video analysis, with an overall CORA rating of 0.79 (Table 2). CORA ratings for all the load cases and impact velocities can be found in the Supplementary Material (Tables S1–S6).

Within the drop test with the rigid neck, all the impact speeds and locations performed similarly as measured using the CORA rating, and the ratings of the individual metrics within impact cases were also similar. Higher CORA rating variability was observed when using the HIII deformable neck, where lower scores were obtained in the impact cases that involved the facemask. Within impact cases, the rotational acceleration of the head demonstrated the lowest correlation ratings (e.g., 0.48) amongst all metrics. Generally, the CORA rating increased with increasing impact speed for the linear and pendulum impacts.

Strain Energy Distribution in Helmet Component Groups

In an exemplary linear impact condition (linear impactor, rear 5.5 m/s), the energy of the impactor mass and initial velocity (232.9 J) was distributed primarily into kinetic energy of the head (26%) followed by the helmet strain energy (20%). The helmet kinetic energy accounted for 17% while the neck strain and kinetic energy accounted for 11% and 7% of the total energy, respectively. The impactor and head strain energy contributed to 16% to the energy distribution. Hourglass and contact energy accounted for the remaining energy balance (3%). The maximum total strain energy of the helmet varied with impact direction and impact speed. The highest total strain energy occurred in rear impact at 39.7 to 66.7 J for impact speeds from 5.5 to 9.3 m/s. The lowest strain energy occurred in the facemask impact (19.1 to 44.5 J for 5.5 m/s to 9.3 m/s).

The HIC_{15} and BrIC values calculated from the head kinematics were plotted against the peak strain energy of each component for all linear impact conditions (Fig. 3). Overall, HIC_{15} was positively correlated with increasing maximum strain energy in each component. The compression shocks exhibited the strongest positive trend (Spearman's $Rho = 0.73$) of increasing HIC_{15} with increasing strain energy, followed by the comfort pads (Spearman's $Rho = 0.70$), shell (Spearman's $Rho = 0.60$), straps (Spearman's $Rho = 0.18$), and facemask (Spearman's $Rho = 0.10$). The increase of BrIC with an increase of maximum strain energy per component was modest and positively correlated with the shell and facemask having the strongest positive correlation (Spearman's $Rho = 0.32$ and 0.31 respectively).

Overall, when the component energies for all impact directions and velocities were averaged, the helmet shell dominated the energy distribution, followed by the compression shocks (Fig. 4). This distribution was particularly pronounced and velocity-independent in configurations where there was no contact between the impactor and facemask. The contribution of the face-

TABLE 2. CORA analysis results.

	Drop tower		Linear impactor		Pendulum
	HIII Head CG and impactor kinematics	NOCSAE Head CG and impactor kinematics	HIII Head CG and impactor kinematics	Helmet rotation	HIII Head CG and impactor kinematics
Overall weighted CORA score	0.88	0.93	0.82	0.79	0.83

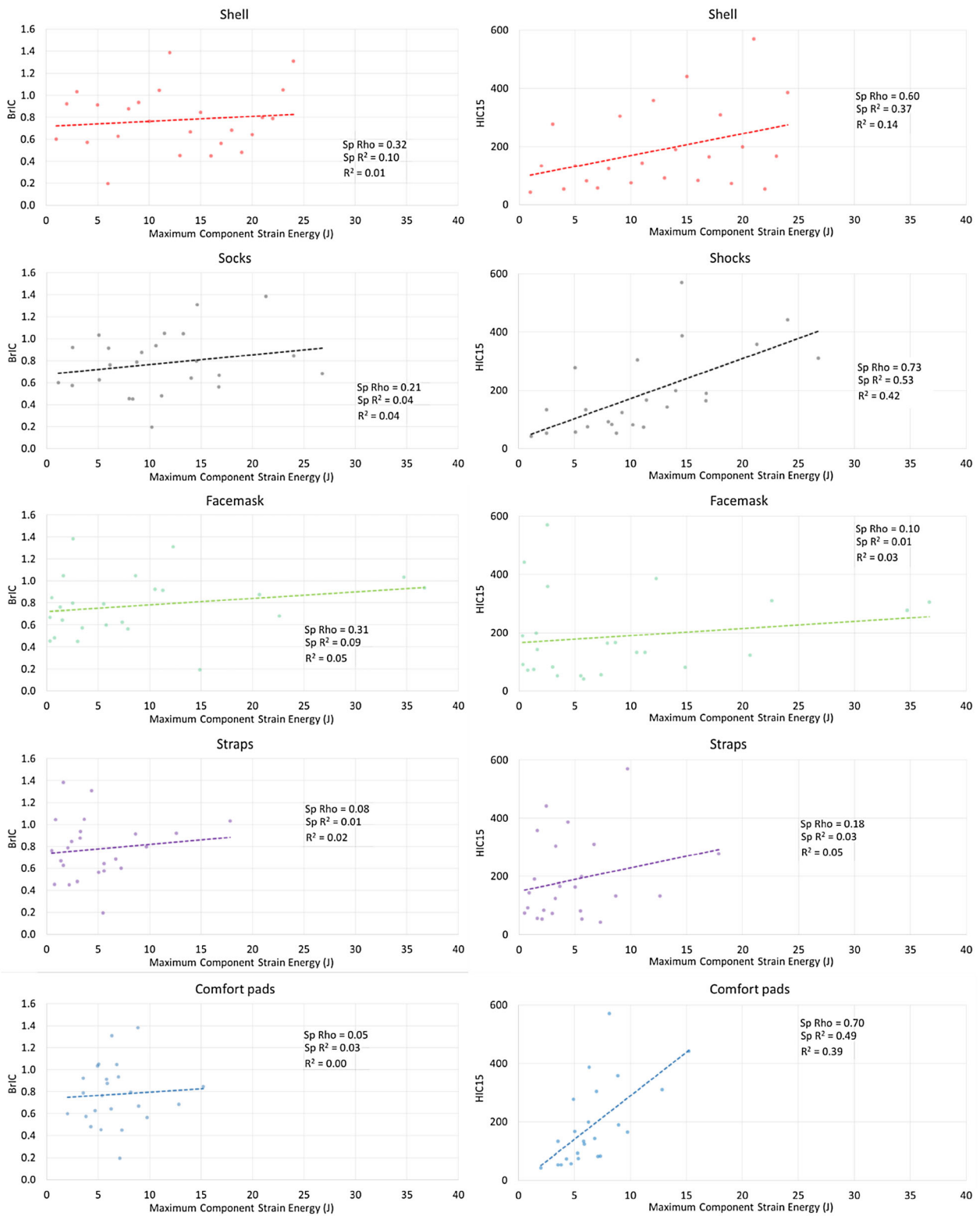


FIGURE 3. BrIC (left) and HIC₁₅ (right) vs. helmet component group strain energy for all linear impact conditions and Spearman's coefficients (Sp Rho), Spearman's R² (Sp R²) and linear regression Coefficient of Determination (R²).

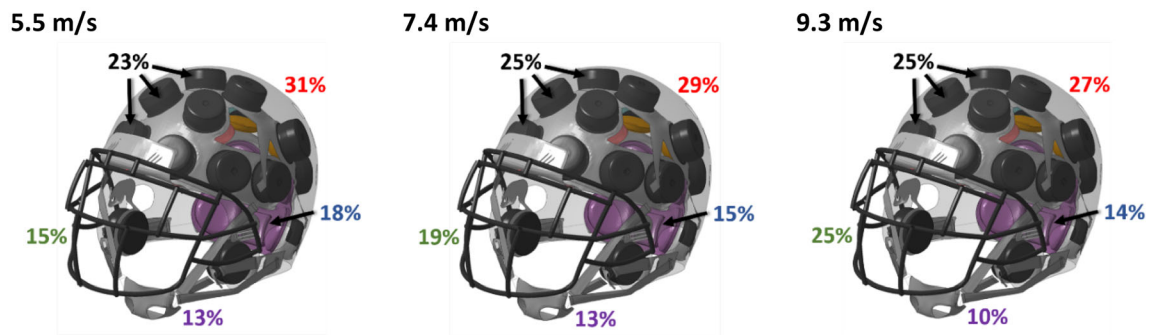


FIGURE 4. Strain energy distribution (Helmet shell in red, shocks in black, facemask in green, comfort pads in blue, and chinstrap in purple), averaged for all impact directions at three impact velocities.

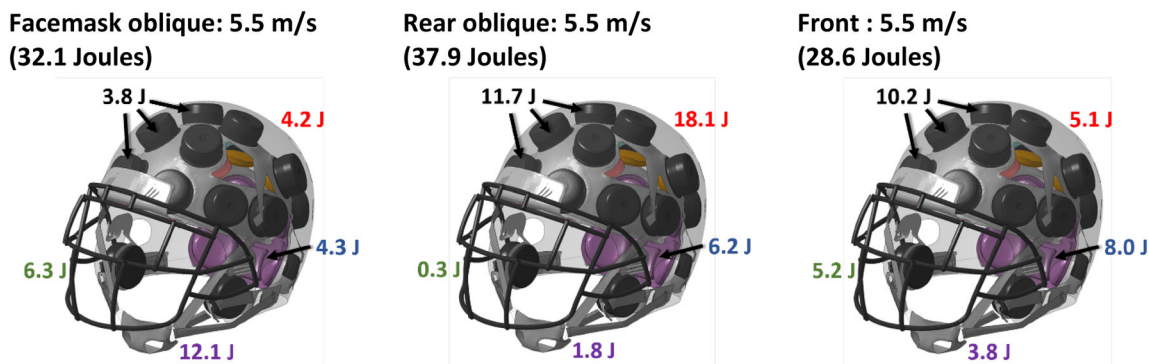


FIGURE 5. Strain energy distribution (helmet shell in red, shocks in black, facemask in green, comfort pads in blue, and chinstrap in purple) for three different impact directions at 5.5 m/s.

mask progressively increased with impact velocity for all impact directions.

For the same impact velocity, the strain energy for each component group was dependent on the impact location. Facemask impacts (Fig. 5a) were primarily absorbed by the strap system while the helmet shell dissipated much of the impact energy when impacted directly at locations distant from the facemask (lateral, rear, and rear oblique) (Fig. 5b). The compression shocks absorbed much of the impact energy under rear oblique, low side, and front top impact configurations (Fig. 5c) that also engaged edges of the facemask. The magnitude of the strain energy in each component group for all impact directions and velocities is summarized in the Supplementary Material (Table S7).

For the same impact direction, the strain energy of each component group changed with increasing impact velocity, which was particularly pronounced in impacts involving the facemask (Fig. 6a). In the oblique facemask impact at 5.5 m/s, the strap system shared 29% of the total strain energy (Fig. 6b); however, at 9.3 m/s strain energy shared by the strap system reached only 12%, falling behind the facemask (33%) and com-

pression shocks (23%) (Fig. 6c). In the facemask lateral impact, the facemask largely dominated the total strain energy distribution (43%), followed by the compression shocks (19%). At lower impact speeds (5.5 m/s) the energy contribution was more equally distributed between the shocks, helmet shell and facemask (21%, 22% and 30% respectively).

DISCUSSION

This study summarized the development and validation of a detailed numerical representation of a modern American football helmet (X2E, 2016, Xenith, LLC). Components of the helmet were previously validated at a material and component level^{1,2} and successfully assembled into a full helmet finite element model using pre-simulation methods to position the deformable internal components (foam, compression shocks) within the helmet shell. The full helmet assembly was donned on the NOCSAE and HIII headforms using a novel headform expansion technique to fit the helmet to the head. Lastly, a strap pre-

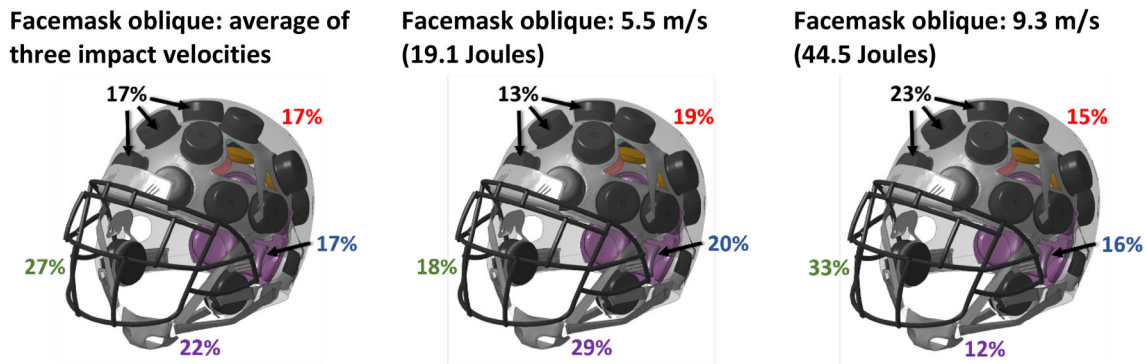


FIGURE 6. Strain energy distribution in component groups for two impact velocities, compared to the average for all impact velocities (helmet shell in red, shocks in black, facemask in green, comfort pads in blue, and chinstrap in purple).

tensioning method was applied to tighten the strap system and fit the helmet to the headform at the start of the simulations, ensuring fit and initial stresses were achieved in the deformable components prior to the impact simulation. Experimental tests of the Xenith X2E helmet were modelled using two validated headforms and impactor models¹¹ and sixty impact configurations were used to validate the assembled full helmet model. A range of impact locations and speeds provided a good assessment of the model performance objectively compared to experimental data, with cross-correlation ratings from good to excellent among the four impact configurations. The lower ratings obtained in the rotational acceleration in the pendulum and linear impact were attributed to the strap-headform interaction, where initial strap tension was not reported in the experimental data.

The helmet component strain energy distribution resulting from impact simulations demonstrated a complicated relationship, depending on both impact location and speed. The helmet shell was found to have the highest strain energy, while the internal deformable structures demonstrated a positive correlation between strain energy and the head injury criterion. The maximum strain energy of each component was positively correlated with HIC_{15} (Fig. 3) for varying impact locations and velocities, where the comfort pads were associated with an increase in HIC_{15} value with increasing strain energy. The increase of HIC_{15} with the strain energy in the comfort pads relative to other components was attributed to the consolidation of the comfort pads for all impact conditions, despite accounting for only 15% of the shared strain energy overall. In contrast, due to the higher energy required to reach consolidation and engagement directly or indirectly through the helmet shell, the compression shocks (strongest correlation between HIC_{15} and strain energy) accounted for 22% of the overall strain energy

for all impact conditions. The correlation of BrIC with increased maximum strain energy was modest when compared to the correlation to HIC_{15} , suggesting a stronger correlation of component deformation to linear kinematics than to rotational kinematics where helmet fitting and impact location could play a substantial role. The low R^2 values suggest a complex relationship between the deformation of each component and the outcome as quantified by HIC_{15} and BrIC. The strain energy share of each component was demonstrated to be dependent on impact velocity (Fig. 4) and impact direction (Fig. 5). Helmet components that were not included in past literature investigations, such as chin cup and straps^{5,14} were found to share a major portion of the strain energy (up to 30%) in impacts engaging the facemask. While an essential contribution of the straps was demonstrated, no information on strap system pre-tension, which could vary significantly depending on the player preference, was available. This factor could influence the energy sharing distribution and requires further investigation.

Limitations of the model included a simplified representation of the straps at locations that were not in contact with the headform (1D beam elements rather than having a 2D elements representation in the entire helmet). The strap system simplifications were based on a common methodology of guiding seatbelts through anchoring points for automotive applications. The sensitivity of strap pretension was not investigated and can potentially affect the deformation of the components as well as head kinematics. Data regarding in-game strap tension is needed for future studies. Also, variations in helmet position on the head were not investigated. In each impact case, the helmet was positioned as reported in the experiments, but variations in orientation could affect the helmet performance. Lastly, the helmet material properties were

measured at room temperature, therefore, the effect of temperature effect on material properties and helmet response was not investigated in the present study.

It was demonstrated that while an energy dissipating structure, such as helmet shell, may dominate the overall model response (Fig. 4), other structures become equally or more critical under different impact directions (Fig. 5). The understanding of how the different components contribute in different impact conditions can inform further development of position-specific helmets since it has been demonstrated that players at different positions were likely to experience impacts from different sources and to different head regions during the game.³⁶ In addition, strain energy shared between the components was impact velocity dependent, highlighting the importance of assessing helmet performance for different impact velocities, which further advances findings of past studies performed at a limited range of impact velocities. The distribution of energy could inform future developments of position-specific helmet designs considering the impact location dependency, and future research should consider optimizing helmet performance for varying impact velocity and location.

ELECTRONIC SUPPLEMENTARY MATERIAL

The online version of this article (<https://doi.org/10.1007/s10439-019-02359-1>) contains supplementary material, which is available to authorized users.

ACKNOWLEDGMENTS

The research presented in this paper was made possible by a grant from Football Research, Inc. (FRI), the National Football League (NFL), and Biomechanical Consulting and Research, LLC (Biocore). The authors acknowledge the contributions of the NFLPA. The views expressed are solely those of the authors and do not represent those of FRI, the NFL, Biocore, or any of their affiliates or funding sources.

REFERENCES

- ¹Barbat, S., Y. Fu, Z. Zhan, and C. Gehre. Objective rating metric for dynamic systems. *Enhanc. Saf. Veh.*, 2013.
- ²Barker, J. B., M. A. Corrales, D. Gierczycka, D. Bruneau, M. C. Bustamante, and D. S. Cronin. Contribution of Energy-absorbing Structures to Head kinematics, 2018.
- ³Biocore, 2018. <http://biocorellc.com/>.
- ⁴Bustamante, M. C., D. Bruneau, J. B. Barker, D. Gierczycka, M. A. Corrales, and D. S. Cronin. Component-level finite element model and validation for a modern American football helmet. *J. Dyn. Behav. Mater.* 5:117–131, 2019.
- ⁵Darling, T., J. Muthuswamy, and S. D. Rajan. Finite element modeling of human brain response to football helmet impacts. *Comput. Methods Biomech. Biomed. Eng.* 19:1432–1442, 2016.
- ⁶Duma, S. M., S. J. Manoogian, W. R. Bussone, P. G. Brolinson, M. W. Goforth, J. J. Donnenwerth, R. M. Greenwald, J. J. Chu, and J. J. Crisco. Analysis of real-time head accelerations in collegiate football players. *Clin. J. Sport Med.* 15:3–8, 2005.
- ⁷Elkin, B. S., L. F. Gabler, M. B. Panzer, and G. P. Siegmund. Brain tissue strains vary with head impact location: a possible explanation for increased concussion risk in struck versus striking football players. *Clin. Biomech.* 64:49–57, 2018.
- ⁸Funk, J., J. Crandall, M. Wonnacott, and C. Withnall. NFL linear impactor helmet test protocol. <http://biocorellc.com/wp-content/uploads/2018/01/NFL-linear-impactor-helmet-test-protocol.pdf>, 2017.
- ⁹Gehre, C., H. Gades, and P. Wernicke. Objective rating of signals using test and simulation responses, 2009.
- ¹⁰Gessel, L. M., S. K. Fields, C. L. Collins, R. W. Dick, and R. D. Comstock. Concussions among United States high school and collegiate athletes. *J. Athl. Train.* 42:495, 2007.
- ¹¹Giudice, J. S., G. Park, K. Kong, A. Bailey, R. Kent, and M. B. Panzer. Development of open-source dummy and impactor models for the assessment of American football helmet Finite element models. *Ann. Biomed. Eng.* 47:464–474, 2019.
- ¹²Greenwald, R. M., J. T. Gwin, J. J. Chu, and J. J. Crisco. Head impact severity measures for evaluating mild traumatic brain injury risk exposure. *Neurosurgery* 62:789–798, 2008.
- ¹³Hoshizaki, T. B., and A. Post. Impact attenuation characteristics of thin walled collapsible air chambers for use in protective helmets. In: Fifth International Symposium on Safety in Ice Hockey, 2010.
- ¹⁴Johnson, K. L., S. Chowdhury, W. B. Lawrimore, Y. Mao, A. Mehmani, R. Prabhu, G. A. Rush, and M. F. Horstemeyer. Constrained topological optimization of a football helmet facemask based on brain response. *Mater. Des.* 111:108–118, 2016.
- ¹⁵Johnston, J. M., H. Ning, J.-E. Kim, Y.-H. Kim, B. Soni, R. Reynolds, L. Cooper, J. B. Andrews, and U. Vaidya. Simulation, fabrication and impact testing of a novel football helmet padding system that decreases rotational acceleration. *Sports Eng.* 18:11–20, 2015.
- ¹⁶King, A. I., K. H. Yang, L. Zhang, and W. Hardy. Is head injury caused by linear or angular acceleration? 2003.
- ¹⁷Kleiven, S. Why most traumatic brain injuries are not caused by linear acceleration but skull fractures are. *Front. Bioeng. Biotechnol.* 1:15, 2015.
- ¹⁸Lamb, L., and T. B. Hoshizaki. Deformation mechanisms and impact attenuation characteristics of thin-walled collapsible air chambers used in head protection. *Proc. Inst. Mech. Eng. Part H* 223:1021–1031, 2009.
- ¹⁹Marar, M., N. M. McIlvain, S. K. Fields, and R. D. Comstock. Epidemiology of concussions among United States high school athletes in 20 sports. *Am. J. Sports Med.* 40:747–755, 2012.

- ²⁰Marjoux, D., D. Baumgartner, C. Deck, and R. Willinger. Head injury prediction capability of the HIC, HIP, SIMon and ULP criteria. *Accid. Anal. Prev.* 40:1135–1148, 2008.
- ²¹Meaney, D. F., and D. H. Smith. Biomechanics of concussion. *Clin. Sports Med.* 30:19–31, 2011.
- ²²National Operating Committee on Standards for Athletic Equipment. Standard Test Method and Equipment Used In Evaluating The Performance Characteristics Of Protective Headgear, 2007.
- ²³NOCSAE. Standard linear impactor test method and equipment used in evaluating the performance characteristics of protective headgear and faceguards, 2019.
- ²⁴NOCSAE. Standard performance specification for newly manufactured football helmets, 2019.
- ²⁵Pellman, E. J., J. W. Powell, D. C. Viano, I. R. Casson, A. M. Tucker, H. Feuer, M. Lovell, J. F. Waeckerle, and D. W. Robertson. Concussion in professional football: epidemiological features of game injuries and review of the literature—part 3. *Neurosurgery* 54:81–96, 2004.
- ²⁶Pellman, E. J., D. C. Viano, A. M. Tucker, I. R. Casson, J. F. Waeckerle, J. C. Maroon, M. R. Lovell, M. W. Collins, D. F. Kelly, A. B. Valadka, R. C. Cantu, J. E. Bailes, and M. L. Levy. Concussion in professional football: reconstruction of game impacts and injuries. *Neurosurgery* 53:799–814, 2003.
- ²⁷Roache, P. J. Perspective: a method for uniform reporting of grid refinement studies. *J. Fluids Eng.* 116:405–413, 1994.
- ²⁸Rowson, S., and S. M. Duma. Development of the STAR evaluation system for football helmets: integrating player head impact exposure and risk of concussion. *Ann. Biomed. Eng.* 39:2130–2140, 2011.
- ²⁹Rowson, S., S. M. Duma, J. G. Beckwith, J. J. Chu, R. M. Greenwald, J. J. Crisco, P. G. Brolinson, A. C. Duhaimé, T. W. McAllister, and A. C. Maerlender. Rotational head kinematics in football impacts: an injury risk function for concussion. *Ann. Biomed. Eng.* 40:1–13, 2012.
- ³⁰Rowson, B., S. Rowson, and S. M. Duma. Hockey STAR: a methodology for assessing the biomechanical performance of hockey helmets. *Ann. Biomed. Eng.* 43:2429–2443, 2015.
- ³¹Schap, J. M., B. Koya, and F. S. Gayzik. Objective evaluation of whole body kinematics in a simulated, restrained frontal impact. *Ann. Biomed. Eng.* 47:512–523, 2019.
- ³²Sproule, D. W., E. T. Campolettano, and S. Rowson. Football helmet impact standards in relation to on-field impacts. *Proc. Inst. Mech. Eng. Part P* 231:317–323, 2017.
- ³³Takhounts, E. G., M. J. Craig, K. Moorhouse, J. McFadden, and V. Hasija. Development of brain injury criteria (Br IC). *Stapp Car Crash J.* 57:243–266, 2013.
- ³⁴Van Der Laan, E., F. Veldpaus, B. De Jager, and M. Steinbuch. Control-oriented modelling of occupants in frontal impacts. *Int. J. Crashworth.* 14:323–337, 2009.
- ³⁵Viano, D. C., C. Withnall, and D. Halstead. Impact performance of modern football helmets. *Ann. Biomed. Eng.* 40:160–174, 2012.
- ³⁶NFL. NFL Safety Tech, Part Two. <<https://www.sporttechie.com/nfl-safety-tech-part-two-engineering-a-safer-sport-with-data/>>.
- ³⁷NFL. Engineering Road Map. <https://www.playsmartplaysafe.com/resource/finite-element-models/>.
- ³⁸Yu, H. Y., B. M. Knowles, and C. R. Dennison. A test bed to examine helmet fit and retention and biomechanical measures of head and neck injury in simulated impact. *J. Vis. Exp.* 127:e56288, 2017.
- ³⁹Zhang, L., D. Ramesh, K. H. Yang, and A. I. King. Effectiveness of the football helmet assessed by finite element modeling and impact testing, 2003.
- ⁴⁰Zhang, L., K. H. Yang, and A. I. King. Biomechanics of neurotrauma. *Neurol. Res.* 23:144–156, 2001.

Publisher's Note Springer Nature remains neutral with regard to jurisdictional claims in published maps and institutional affiliations.